

Si(111)-(7×7) surface probed by reflection high-energy positron diffraction

A. Kawasuso,* Y. Fukaya, K. Hayashi, M. Maekawa, S. Okada, and A. Ichimiya

Advanced Science Research Center, Japan Atomic Energy Research Institute, 1233 Watanuki, Takasaki, Gunma 370-1292, Japan

(Received 20 October 2003; published 31 December 2003)

We report the observation of reflection high-energy positron diffraction from a 7×7 reconstructed Si(111) surface with a well-collimated 20-kV positron beam. The diffraction pattern clearly exhibited the $(1/7)-(3/7)$ order Laue zones in addition to the zeroth and first Laue zones. From the dynamical calculation of the rocking curve in the total reflection region, the vertical position of adatom layer was determined to be 1.52 \AA relative to the stacking fault layer. This value is greater than that predicted in the first-principles study suggesting a significant outward relaxation of adatoms.

DOI: 10.1103/PhysRevB.68.241313

PACS number(s): 61.14.Hg, 68.35.Bs

In this paper, we demonstrate the observation of reflection high-energy positron diffraction (RHEPD) from a Si(111)-(7×7) surface. The rocking curve (intensity versus glancing angle) of totally reflected positrons is carefully analyzed using the dynamical diffraction theory. The vertical positions of adatoms in the dimmer-adatom-stacking-fault (DAS) structure are precisely determined with a minimum influence from the inner structure.

The atomic arrangement of the 7×7 reconstructed Si(111) surface was fully determined by direct observation using a scanning tunneling microscope and Patterson analysis of the transmission electron-diffraction pattern.^{1,2} These confirmed the DAS structure proposed by Takayanagi *et al.*² for Si(111)-(7×7) surface. Meanwhile, the interlayer distances in the DAS structure were determined in low-energy electron diffraction (LEED),³ reflection high-energy electron diffraction (RHEED),⁴ and x-ray diffraction (XRD).⁵ The obtained interlayer distances are more or less in good agreement with those obtained by the first-principles calculations.^{6,7} However, the position of the adatom layer determined by XRD is likely to be overestimated.⁵ The phase transition of Si(111)-(7×7) surface at high temperatures⁸ is dominated by thermal properties of adatoms. It is important to know the vertical position of adatoms. However, the above discrepancy has not yet been revealed.

Since the establishment of RHEPD, it has been shown that the total reflection positron diffraction has the capability to measure small surface atomic displacements with a precision of 0.01 nm .⁹⁻¹¹ It is known that x rays are also totally reflected at crystal surfaces. This property is thought to be useful in determining atomic arrangements at the surface. Characteristic differences between positrons and x rays are due to their penetration depths and reflectivities. Due to the rapid extinction of the incident positron wave, positrons probe much shallower regions (a few angstroms) than x ray (typically $> 100 \text{ \AA}$). Strong interaction between positrons and nuclei results in more than three orders of magnitude greater reflectivity as compared to x ray. The multiple-scattering processes must be accounted for when analyzing RHEPD rocking curve and pattern. Nevertheless, the bond length of atoms on surface can be approximately estimated from the fine structures in the rocking curve. For instance, if adatoms exist on a surface, an absorptive peak or a discontinuity is observed in the rocking curve. The location of dis-

continuity can be used to calculate the bond length of adatoms. Thus, RHEPD rocking curve appears to be more sensitive than x rays for examining the surface region.

With the above facts in mind, we have observed the positron diffraction from a Si(111)-(7×7) surface. We precisely measured the rocking curve and extracted the vertical positions of adatoms.

The sample used in this study was a phosphorus doped *n*-type Si(111) wafer with a resistivity of 10 \Omega cm ($15\times 5\times 0.5 \text{ mm}^3$). After the surface cleaning with an acetone and ultrapure water, the sample was transferred into a vacuum chamber evacuated to a base pressure of $6\times 10^{-8} \text{ Pa}$. The sample flashing was done by a direct current flow ($\sim 14 \text{ A}$) for a few seconds and by cooling down slowly to avoid the surface defect formation. This flashing method is ordinarily employed to form a 7×7 reconstructed surface. A 20-keV well-collimated positron beam with a flux of 2×10^3 positrons/s was generated by an electrostatic positron beam described elsewhere.¹⁰ The sample surface was irradiated with the beam and backscattered positrons were detected using a Hamamatsu F2226-24P multichannel plate assembly (MCPA) containing a phosphor plane. The phosphor plane images of scattered positrons were observed by a computer-controlled charge-coupled device camera. The image frames were digitally integrated with a rate of 30 s^{-1} . The rocking curve of specularly reflected positrons was measured as a function of glancing angle from 0.5° to 4.2° with 0.1° step. Details of the apparatus were described elsewhere.¹²

Although the beam intensity was rather low, the energy and angular divergences were less than 0.1% and 0.1° , respectively.¹³ The Si(111)-(7×7) surface has seven times greater lattice constant ($=3.84\times 7\sim 30 \text{ \AA}$) as compared to the bulk truncated surface. To observe it, the coherence length of the positron beam should be long enough. The coherence length parallel to the surface is given by $24.5E^{1/2}/\Delta E$, where E and ΔE are the respective beam energy and its spread. Thus, the coherence length of the present beam is $\approx 170 \text{ \AA}$ and hence adequate to observe a 7×7 reconstructed surface.

Figure 1 shows the RHEPD pattern obtained for incidence of the $[11\bar{2}]$ and a glancing angle of 1.5° after the image accumulation for over 8 h. The glancing angle chosen here is very close to the condition satisfying the first Bragg reflec-

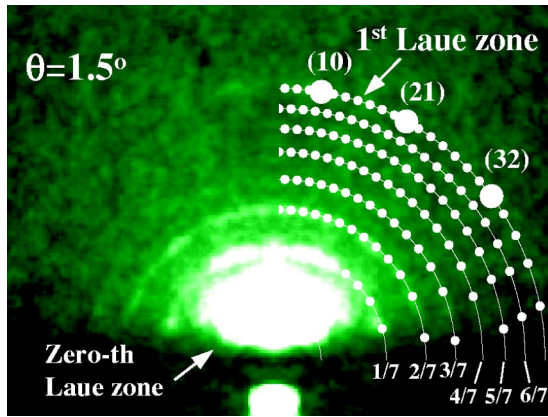


FIG. 1. Reflection high-energy positron diffraction pattern from a Si(111)-(7 \times 7) surface at the [11 $\bar{2}$] incidence and glancing angle of 1.5 $^\circ$. Incident positron energy is 20 keV. The Laue zone and spot positions expected from a 7 \times 7 reciprocal lattice are schematically shown on the right.

tion. It is seen that three obvious ring patterns exist between the zeroth and the first Laue zones. To confirm that these patterns are coming from the 7 \times 7 reconstructed surface, the spot positions calculated from the kinematical theory are also shown. From this agreement, three ring patterns are assigned to 1/7–3/7 Laue zones. The 4/7–6/7 Laue zones were not clearly seen by eye. To visualize these weak patterns more clearly, we need to enhance the beam intensity furthermore so as to overcompensate the dark current from the MCPA. The observed variation of the fractional order spots in the same ring pattern will be investigated using the dynamical diffraction theory more in detail taking into account of the atomic configuration of the DAS structure.

Figure 2(a) shows the rocking curve of the specular spot at 7.5 $^\circ$ away from the [11 $\bar{2}$] direction (one-beam condition). In this geometry, the rocking curve depends only on the vertical positions of atomic layers near the surface region.⁴ The specular intensity increases from 0.5 $^\circ$ until a peak at 1.6 $^\circ$. A small shoulder at 2.2 $^\circ$ and two more peaks at 2.7 $^\circ$ and 3.4 $^\circ$ are also noted. The critical glancing angle for the total reflection is calculated by $\theta_C = \arcsin(V_0/E)^{1/2}$, where V_0 denotes the crystal potential.¹⁴ Taking $V_0 = 12$ eV from the Doyle and Turner table,¹⁵ we obtain $\theta_C = 1.4^\circ$. The Bragg condition is given by $E \sin^2 \theta = 37.5n^2/d^2 + V_0$ (n , integer; d , bilayer distance = 3.14 Å). Thus, the region up to 1.4 $^\circ$ corresponds to the total reflection. The peak at 1.6 $^\circ$ originates from the (111) Bragg reflection. Furthermore, the peaks at 2.2 $^\circ$, 2.7 $^\circ$, and 3.4 $^\circ$ can be assigned to the (222), (333), and (444) Bragg reflections, respectively.

The intensity distribution below 1.6 $^\circ$ reflects the condition of the surface. Absence of any absorption loss in this region indicates that the surface is atomically smooth. However, the slope of the curve changes at around 1.1 $^\circ$ as noted in the figure. To confirm the existence of the small discontinuity, we have repeated this experiment several times, each giving the same results. The discontinuity is due to the existence of adatoms, i.e., the interference and inelastic-scattering effects among positron waves reflected at the adatom layer and the next layer below it. The relative heights on

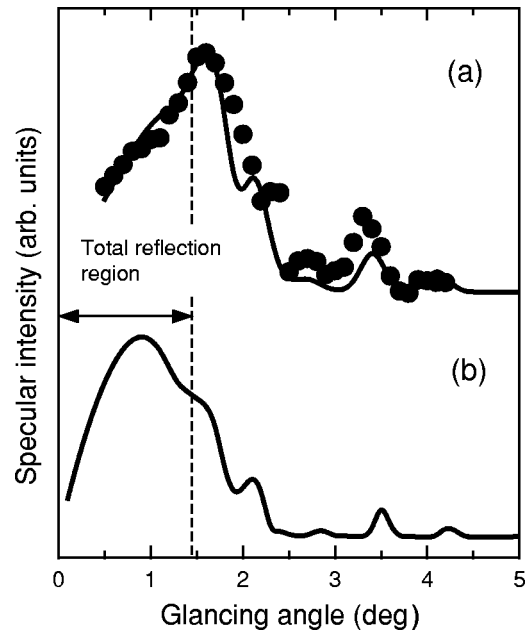


FIG. 2. (a) Filled circles show the experimental rocking curve of specularly reflected positrons in the one-beam condition (7.5 $^\circ$ away from the [11 $\bar{2}$] direction) with an incident positron energy of 20 keV. Solid line exhibits the best rocking curve calculated using the dynamical theory by adjusting the distance between adatom and stacking fault layers and absorption potential due to electronic excitation. (b) Rocking curve calculated using the parameters determined in the previous RHEED study (see text).

either side of the discontinuity increase when the position of the adatom relaxes further into the bulk region and thereby suppresses interference effect.

We attempted to reproduce the experimental rocking curve using the dynamical calculation¹⁶ and to extract the vertical position of adatoms. In the calculation, the crystal potential was expressed as a complex potential ($=V_0 + iV'$). The imaginary part describes the inelastic damping, which is composed of the phonon scattering potential V_{ph} and the electronic excitation potential V_e . Thermal vibration of atoms was described using the Debye parameter. The layer sequences in the DAS structure were assumed as shown in Fig. 3.

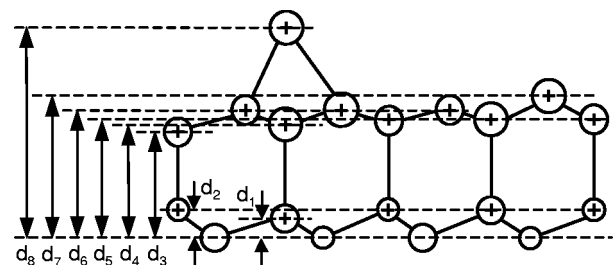


FIG. 3. Definition of interlayer distances in the dimer-adatom-stacking fault structure (only the unfaulted half is shown for simplicity). d_1 and d_2 , d_3 – d_5 , d_6 and d_7 , and d_8 are the relative distances of atoms in the bulk layer, the dimer layer, stacking fault layer, and adatom layer, respectively, to the fourth layer. The distance between adatom and stacking fault layer is given by $d_{ad} = d_8 - d_6$.

TABLE I. Mean spacings between adatom and stacking fault layers (d_{ad}) determined in the present and previous studies.

Present (Å)	XRD ^a (Å)	RHEED ^b (Å)	LEED ^c (Å)	Theory ^d (Å)
1.52	1.58	1.28, 1.44	1.23	1.34

^aNote Ref. 5.

^bNote Refs. 4 and 8.

^cNote Ref. 3.

^dNote Ref. 7.

The interlayer distance determined in the previous electron diffraction and theoretical studies coincide to within 0.1 Å.^{3,4,7} In the case of XRD, the adatom position was found to be shifted away from the surface. Initially, the rocking curves were calculated using the atomic configurations determined by using RHEED and theory.^{4,7} These results were nearly the same after including the same Debye parameter and the crystal potential. Figure 2(b) shows the rocking curve calculated using the same conditions as in the RHEED study.⁴ It is readily seen that the calculated and experimental rocking curves are in good agreement at $\theta > 2.0^\circ$. However, in the total reflection region and around the first Bragg peak (1.6°), the agreement is not as good since the calculation was optimized to reproduce the features of the higher-order Bragg reflections which are sensitive to the atomic configuration in relatively deep regions. With electron diffraction it is rather difficult to determine the atomic configuration of the first monolayer due to the influence from the interior.

To reproduce the experimental rocking curve, the interlayer distance, the absorption potential, and the Debye parameter used in the RHEED study should be modified. During the initial calculations, we found that the rocking curves were quite sensitive to the relative distance between adatom and stacking fault layers ($d_{ad} = d_8 - d_6$) and not to the shift of the other atomic layers ($d_1 - d_5$ and d_7). It was also found that the changes in the Debye parameter and absorption potential due to the thermal diffuse scattering resulted in minor effects to the curve shape in the total reflection region. Thus, the distance between the adatom and stacking fault layers and the absorption potential due to electronic excitations (V_e) were varied so as to reproduce the experimental rocking curve. The other interlayer distances were fixed at the same values obtained from the electron diffraction.⁴ The Debye parameter and the absorption potential for thermal diffuse scattering were fixed at 0.3 \AA^2 and 0.2 eV , respectively. The solid line in Fig. 2(a) is the best calculated rocking curve. The optimum distance between adatom and stacking fault layers and the electronic absorption potential were determined to be $d_{ad} = 1.52 \text{ \AA}$ and $V_e = 0.25 \text{ eV}$, respectively. The Pendry R -factor was estimated to be 0.17 suggesting that the experimental curve is well reproduced.

Table I lists the d_{ad} values obtained in the present and

previous studies. Early electron-diffraction studies^{3,4} suggest $d_{ad} = 1.23 - 1.28 \text{ \AA}$, which is comparable to the result of the first-principles calculation ($d_{ad} = 1.34 \text{ \AA}$).⁷ Recent more detailed RHEED study has reported a greater value ($d_{ad} = 1.44 \text{ \AA}$).⁸ The XRD study gives a remarkably high value ($d_{ad} = 1.58 \text{ \AA}$).⁵ The present value ($d_{ad} = 1.52 \text{ \AA}$) is shifted to 0.18 \AA from that expected by theory. It has long been thought that XRD overestimates the distance between the adatom and stacking fault layers. However, the present results indicate that the d_{ad} determined by XRD study is not necessarily unrealistic. Thus, the distance between the adatom and stacking fault layers should be within the range from 1.52 to 1.58 \AA .

The deviation of d_{ad} from that calculated using the first principles is not clear at present. One possible explanation may be the different temperatures used in calculation and experiment; that is, the present diffraction experiment was carried out at room temperature, while the theory assumes 0 K . It is suggested that the adatom bond is softened as compared to the bulk atoms.¹⁷ The soft adatom bond is thought to dominate the migration of adatoms and initiate phase transition from the 7×7 to 1×1 reconstructions at 1100 K . Also, the electron energy-loss features at low temperatures¹⁸ might be better understood by considering the anharmonicity of the adatom bond. It is therefore anticipated that the value of d_{ad} approaches the ideal theoretical value at low temperatures.

The absorption potential due to the electronic excitation obtained above is approximately half of that anticipated from the RHEED (Ref. 4) and the theory based on the bulk plasmon excitation.¹⁹ Since the cross section of plasmon excitation itself should be quite similar for electrons and positrons, the smaller absorption potential may be interpreted as a lack of bulk plasmon excitation due to incident positrons. Probably, incident positrons are reflected mostly at the topmost surface and hence the surface plasmon excitation with a smaller energy may be more efficient as compared to the bulk plasmon excitation with a larger energy.

In conclusion, we have confirmed the high-energy positron diffraction from a Si(111)-(7×7) surface. The rocking curve of the specularly reflected positrons was determined in the one-beam condition. It was found that the intensity distribution of totally reflected positrons was sensitive to the distance between adatom and stacking fault layers and to the electronic absorption potential. A detailed analysis based on the dynamical theory revealed that the adatom layer undergoes a greater outward relaxation than that expected from first-principles calculation. The distance between adatom and the first layer can be determined precisely by RHEED and XRD. A shift of interlayer distances in the subsurface region is observed (several atomic layers) by RHEED and LEED.

This work was partly promoted as the Nuclear Energy Fundamentals Crossover Research in the Ministry of Education, Culture, Sports, Science and Technology of Japan.

*Electronic address: ak@taka.jaeri.go.jp

¹G. Binnig, H. Rohrer, C. Gerber, and E. Weibel, Phys. Rev. Lett. **50**, 120 (1983).

²K. Takayanagi, Y. Tanishiro, S. Takahashi, and M. Takahashi,

Surf. Sci. **164**, 367 (1985).

³H. Huang, S.Y. Tong, W.E. Packard, and M.B. Webb, Phys. Lett. A **130**, 166 (1987).

⁴A. Ichimiya, Surf. Sci. **192**, L893 (1987).

- ⁵I.K. Robinson and E. Vlieg, *Surf. Sci.* **261**, 123 (1987).
- ⁶G.-X. Qian and D. Chadi, *Phys. Rev. B* **35**, 1288 (1987).
- ⁷K.D. Brommer, M. Needels, B.E. Larson, and J.D. Joannopoulos, *Phys. Rev. Lett.* **68**, 1355 (1992).
- ⁸Y. Fukaya and Y. Shigeta, *Phys. Rev. Lett.* **85**, 5150 (2000).
- ⁹A. Kawasuso and S. Okada, *Phys. Rev. Lett.* **81**, 2695 (1998).
- ¹⁰A. Kawasuso, S. Okada, and A. Ichimiya, *Nucl. Instrum. Methods Phys. Res. B* **171**, 219 (2000).
- ¹¹A. Kawasuso, M. Yoshikawa, K. Kojima, S. Okada, and A. Ichimiya, *Phys. Rev. B* **61**, 2102 (2000).
- ¹²T. Ishimoto, A. Kawasuso, and H. Itoh, *Appl. Surf. Sci.* **194**, 43 (2002).
- ¹³A. Kawasuso, T. Ishimoto, S. Okada, H. Itoh, and A. Ichimiya, *Appl. Surf. Sci.* **194**, 287 (2002).
- ¹⁴A. Ichimiya, *Solid State Commun.* **28**, 143 (1992).
- ¹⁵P.A. Doyle and P. Turner, *Acta Crystallogr.* **24**, 390 (1967).
- ¹⁶A. Ichimiya, *Jpn. J. Appl. Phys., Part 2* **22**, 176 (1983).
- ¹⁷I. Štich, J. Kohanoff, and K. Terakura, *Phys. Rev. B* **54**, 2642 (1996).
- ¹⁸W. Daum, H. Ibach, and J.E. Müller, *Phys. Rev. Lett.* **59**, 1593 (1987).
- ¹⁹G. Radi, *Acta Crystallogr., Sect. A: Cryst. Phys., Diffr., Theor. Gen. Crystallogr.* **26**, 41 (1970).